In Situ Analysis of Changes in Telomere Size during Replicative Aging and Cell Transformation

Scott Henderson,* Richard Allsopp,‡§ David Spector,* Sy-Shi Wang‡ and Calvin Harley‡

*Cold Spring Harbor Laboratory, Cold Spring Harbor, New York 11724; ‡Geron Corp., Menlo Park, California 94025; and §McMaster University, Hamilton, Ontario Canada L8N 325

Abstract. Telomeres have been shown to gradually shorten during replicative aging in human somatic cells by Southern analysis. This study examines telomere shortening at the single cell level by fluorescence in situ hybridization (FISH). FISH and confocal microscopy of interphase human diploid fibroblasts (HDFs) demonstrate that telomeres are distributed throughout the nucleus with an interchromosomal heterogeneity in size. Analysis of HDFs at increasing population doubling levels shows a gradual decrease in spot size, intensity, and detectability of telomeric signal. FISH of metaphase chromosomes prepared from young and old HDFs shows a heterogeneity in detection frequency for telomeres on chromosomes 1, 9, 15, and Y. The interchromosomal distribution of detection frequencies was similar for cells at early and late passage. The telomeric detection frequency for metaphase chromosomes also decreased with age. These observations suggest that telomeres shorten at similar rates in normal human somatic cells. T-antigen transformed HDFs near crisis contained telomere signals that were low compared to nontransformed HDFs. A large intracellular heterogeneity in telomere lengths was detected in two telomerase-negative cell lines compared to normal somatic cells and the telomerase-positive 293 cell line. Many telomerase-negative immortal cells had telomeric signals stronger than those in young HDFs, suggesting a different mechanism for telomere length regulation in telomerase-negative immortal cells. These studies provide an in situ demonstration of interchromosomal heterogeneity in telomere lengths. Furthermore, FISH is a reliable and sensitive method for detecting changes in telomere size at the single cell level.

NORMAL eukaryotic somatic cells can only undergo a finite number of divisions in vitro, also known as the Hayflick limit. This phenomenon was originally described as senescence at the cellular level over 30 years ago (Hayflick and Moorhead, 1961), and has now been established as a senescence process in higher eukaryotes (Martin et al., 1970; Dell'Orco et al., 1973; Goldstein, 1974; for reviews see Stanulis-Praeger, 1987; Finch, 1990; Goldstein, 1990). Numerous models have been proposed to explain the cause(s) of cell senescence (for reviews see Stanulis-Praeger, 1987; Finch, 1990; Goldstein, 1990). One of these models is based upon the loss of telomeric DNA that occurs during replicative aging of somatic cells, which provides an intrinsic biological clock to explain cell senescence (Harley, 1991).

Telomeres are physical elements located at the ends of all eukaryotic chromosomes and are essential for genetic stability (Muller, 1938; McClintock, 1941; Lundblad and Szostak, 1989; for reviews see Blackburn, 1991; Gilson et al., 1993; Sandell and Zakian, 1993). Telomeres differentiate chromosome ends from double-stranded DNA breaks and protect them from nuclease degradation or aberrant recombination (Muller, 1938; McClintock, 1941; Henderson et al., 1990; Bourgain and Katinka, 1991). Telomeres may also play a role in the subnuclear organization of chromatin (for review see Gilson et al., 1993) and may facilitate chromosome pairing during meiosis (Sen and Gilbert, 1988). Telomeres are composed of specialized chromatin (Tommerup et al., 1994; Blackburn, 1991), the DNA component of which consists of repetitive sequences that are G-rich in the 5′→3′ strand (Blackburn, 1991). The telomeric DNA sequence of vertebrates is (TTAGGG)n (Meyne et al., 1989). The terminal restriction fragment (TRF)[1] length of DNA from normal somatic cells from young adults is typically in the 8–10-kbp range in adults (de Lange et al., 1990; Harley et al., 1990; Hastie et al., 1990; Vaziri et al., 1993). However, 4–5 kbp of the TRF in normal cells are estimated to be composed of nontelo-

Please address all correspondence to S. Henderson, Mount Sinai School of Medicine, Department of Cell Biology and Anatomy, Box 1007, One Gustave L. Levy Place, New York, NY 10029. Tel.: (212) 241-5018. Fax: (212) 860-1174.

S. Henderson and R. Allsopp contributed equally to this work.

1. *Abbreviations used in this paper*: HDF, human diploid fibroblast; FISH, fluorescence in situ hybridization; PDL, population doubling time; TRF, terminal restriction fragment.

meric and telomere-like sequences (Allshire et al., 1989; Brown et al., 1990; de Lange et al., 1990; Weber et al., 1990; Wells et al., 1990; Levy et al., 1992). Thus, the length of the terminal TTAGGG tract (i.e., telomeric DNA length) in these cells is ~6–3 kbp (see Fig. 1 *A*).

Without a special mechanism to complete telomere replication, the ends of chromosomes are predicted to gradually shorten with replicative age (Olovnikov, 1971, 1973). This hypothesis was based upon the inability of the DNA replication machinery to completely replicate the ends of linear DNA molecules (Watson, 1972; for review see Blackburn, 1991). Recently, this hypothesis has been shown to be correct in studies by us and others which have revealed that the amount of telomeric DNA decreases during replicative aging of various human somatic cell types both in vitro and in vivo (Harley et al., 1990; Hastie et al., 1990; Lindsey et al., 1991; Allsopp et al., 1992; Counter et al., 1992; Vaziri et al., 1993, 1994; Chang and Harley, 1995; Weng et al., 1995). These observations are consistent with the telomere hypothesis of cell aging (Harley, 1991), which proposes that the shortening of one or more telomeres below a certain length (Tc) critical for proper telomere structure and function will induce irreversible cell cycle arrest (cell senescence or the M1 checkpoint) (see Fig. 1 *B*).

Telomere length is maintained in immortal cell populations including the germ line by telomerase, a protein/RNA complex capable of synthesizing telomeric DNA de novo (Greider and Blackburn, 1985; for review see Blackburn, 1991). The RNA component of telomerase contains a short motif which corresponds to the telomeric DNA sequence and which provides a template for the addition of telomeric DNA onto the 3′ terminus of chromosomal ends (Greider and Blackburn, 1989; Feng et al., 1995). Telomerase has been detected in various human cell lines and tumor tissue (Counter et al., 1992; Counter et al., 1994*a*,*b*; Kim et al., 1994), as well as human germ line tissue (Kim et al., 1994) and appears to be either absent or present at very low levels in most adult somatic tissues (Counter et al., 1992; Kim et al., 1994; Broccoli et al., 1995; Chiu et al., 1996; Counter et al., 1995; Hiyama et al., 1995). After transformed cells have bypassed cell senescence, telomere length continues to shorten and the frequency of dicentric chromosomes formed via end to end fusion increases until cells reach crisis (i.e., M2 checkpoint; Fig. 1 *B*) (Counter et al., 1992, 1994*a*). These observations have led to the suggestion that telomere shortening may also have a causal role in crisis (Harley, 1991; Wright and Shay, 1995). In addition, in transformed human cells which have acquired the ability to bypass the M1 checkpoint, the expression of telomerase has been shown to coincide with the maintenance of telomere length, suggesting that telomerase is essential for immortalization (i.e., the survival beyond crisis or the M2 checkpoint when most cells die) (Counter et al., 1992, 1994*a*). Recently, a small number of human cell lines which have no detectable telomerase activity have been identified (Kim et al., 1994; Murnane et al., 1994; Bryan et al., 1995). The mechanism of telomere length maintenance in these special cases has yet to be determined.

All of our previous analyses of telomeric DNA length have used Southern hybridization with a telomere-specific probe. However, it is not possible to analyze the lengths of individual telomeres by this technique due to the heterogeneity in telomere length that exists in a cell population. In this study, we have used fluorescence in situ hybridization (FISH) to evaluate the relative loss of telomeric DNA from individual chromosomal ends on an individual cellular basis during replicative aging of normal and transformed human fibroblasts.

Materials and Methods

Cell Culture

BJ cells (fetal male human foreskin fibroblast), S2C cells (adult skin fibroblast), IMR90 cells (female human lung diploid fibroblast; Amer. Type Culture Collection, Rockville, MD No. CCL 186), SW26 cells (SV40-transfected IMR90 cells at precrisis stage), and SW26i cells (stable postcrisis immortal line from SW26) were cultured in DMEM/M199 (4:1) (GIBCO/BRL, Gaithersburg, MD) supplemented with either 10% FBS or 10% BCS and 1% penicillin/streptomycin or 1% gentamycin, respectively. WI-38 cells (female human lung diploid fibroblast; ATCC No. CCL 35) were cultured in MEM supplemented with 10% FBS and 1% penicillin/streptomycin. WI38-VA13 cells (SV40-transformed human WI-38 fibroblasts; ATCC #CCL 75.1) were cultured in DMEM supplemented with 10% FBS and 1% penicillin/streptomycin.

For interphase FISH analysis of human fibroblast strains and transformed cell lines, cells were plated and grown on 22-mm^2 acid-washed glass coverslips (1.5 thickness) in 35-mm culture dishes.

Probes

For interphase FISH analysis, a genomic telomere probe (pHuR93/ATCC No. 61076; Moyzis et al., 1988) and a probe to the subtelomeric region of the long arm of chromosome 13 (pEE3A; Murnane and Yu, 1993) were labeled with either biotin-16-dUTP (Boehringer Mannheim Corp., Indianapolis, IN), digoxigenin-11-dUTP (Boehringer Mannheim), fluorescein-12-dUTP (Boehringer Mannheim), or tetramethyl-rhodamine-6-dUTP (Boehringer Mannheim) by nick translation (Langer et al., 1981). A digoxigenin-labeled probe for the subtelomeric region of the long arm of chromosome 14 (Tel 14q; cat. No. P5428-DIG) was purchased from Oncor (Gaithersburg, MD). For FISH analysis of metaphase chromosomes, the telomeric probe pBLrep4 (a PCR-generated $(TTAGGG)_n$ probe of ~600 bp, provided by W. Wright and J.W. Shay, University of Texas Southwestern Medical Center, Dallas, TX) labeled with either biotin-16-dUTP or digoxigenin-11-dUTP was used.

In Situ Hybridization and Detection

Interphase Nuclei. Cells grown on coverslips in 35-mm culture dishes were rinsed briefly in PBS, pH 7.4, and then fixed in 2.5% formaldehyde plus 5 mM $MgCl_2$ in PBS, pH 7.4, for 10 min at room temperature. After fixation, the cells were washed three times (10 min each) with 0.3 M glycine in PBS, pH 7.4, permeabilized with 0.2% Triton X-100 in PBS for 5 min, and then washed three times (10 min each) in PBS, pH 7.4. To preserve nuclear morphology, hypotonic swelling, cell lysing, ethanol dehydration, and air drying, steps commonly employed during in situ hybridization protocols, were not used.

The cells were then washed with 2× SSC at room temperature before denaturation of cellular DNA in 70% deionized formamide in 2 × SSC at 80°C for 10 min. After denaturation, the cells were washed immediately with ice-cold 70% deionized formamide in 2 × SSC followed by a wash in 2× SSC.

Labeled telomere probe (100 ng in a 10-μl vol of 1× SSC) was dried in a SpeedVac (Savant DNA 100), and then resuspended in 10 μl of 100% deionized formamide. For double label studies, the labeled telomere probe was dried along with 400 ng (in a 10-μl vol of 1× SSC) of labeled pEE3A and resuspended in 10 μl of 100% deionized formamide. The probes were denatured by heating in an 80°C waterbath for 10 min and then were placed immediately on ice. Hybridization buffer was added to

each probe to give a final volume of 20 μl and a final concentration of 50% formamide, 2× SSC, 2× Denhardt's solution, 10% dextran sulfate, and 50 mM Tris, pH 7.5. In other double label studies, the telomere probe was dried and resuspended in 5 μl of 100% deionized formamide, denatured, placed in a 10-μl volume of hybridization buffer, and added to 10 μl of Oncor Tel 14q probe in hybridization buffer (20 μl final volume).

The probes in hybridization buffer (20 μl total volume) were added to the cells on coverslips, inverted onto glass microscope slides, and sealed with rubber cement. After incubation overnight at 37°C, the coverslips were washed twice (30 min each) in 50% formamide in 2× SSC at 37°C and then washed (30 min) in 2× SSC at 37°C followed by washes at room temperature in 2× SSC.

The coverslips were then incubated for 60 min at room temperature in 2× SSC plus 1% BSA plus one or more of the following: fluorescein avidin DN (5 μg/ml) (Vector Laboratories Inc., Burlingame, CA), and FITC- or rhodamine-conjugated anti-digoxigenin antibodies (50 μg/ml) (Boehringer Mannheim). No further amplification of signal was used for interphase FISH analysis. After labeling, the cells were washed for 5 min each with 2× SSC, followed by PBS, 0.1% Triton X-100 in PBS, and finally three washes with PBS, pH 7.4. Coverslips were mounted in 9:1 glycerol: PBS containing 0.1% *p*-phenylenediamine buffered to pH 8.0 with 0.5 M carbonate/bicarbonate buffer (Johnson and Nogueira Araujo, 1981).

Cells were imaged with a Zeiss confocal laser scanning microscope, equipped with a 100×/1.3 NA oil immersion lens, an Argon Ion laser (λ = 488 nm) and a Helium/Neon laser (λ = 543 nm).

Metaphase Chromosomes. Metaphase spreads were prepared using standard methanol/acetic acid fixation methods. DNA was denatured by immersing slides in 70% deionized formamide/2× SSC heated to 72°C for 2.5 min. After denaturation, slides were immediately transferred through a series of ice-cold ethanol washes (70%, 95%, and 100% solutions; 3 min each) and then allowed to air dry. 120 ng of telomeric probe was dried down and resuspended in formamide and denatured as described above.

When using a biotinylated telomeric probe, the hybridization protocol and subsequent washes were essentially done as described above for interphase cells, except that the posthybridization washes were done at 44°C and for 5 min each. Also, the fluorescent signal was amplified by incubating the slides at RT in PNM buffer (0.1 M phosphate, pH 8.0/0.1% NP-40 plus 5% dried milk powder) containing 5 μg/ml biotinylated antiavidin (Vector Laboratories Inc.) for 20 min. The slides were then washed (5 min each) in 4× SSC, 4× SSC/0.1% Triton X-100, 4× SSC, PN buffer (PNM buffer without dried milk powder). The slides were incubated once more with FITC-avidin in PNM buffer (final concentration, 5 μg/ml) at RT for 20 min followed by the same wash steps used to remove unbound biotinylated antiavidin. DAPI/distamycin A (DA) staining was then performed as described by Schweizer et al. (1978). DAPI and nonfluorescent DA both bind preferentially, but with different affinities, to A-T rich DNA sequences (Schweizer et al., 1978). Because DA is nonfluorescent, it obliterates DAPI fluorescence at all chromosomal regions except at certain constitutive heterochromatic regions at the constrictions of chromosomes 1, 9, 16, the short arm of chromosome 15 and the long arm of the Y chromosome, thus allowing the specific identification of these chromosomes. Slides were mounted in antifade mounting medium (as described above) containing 0.8 μg/ml propidium iodide.

When using a digoxigenin-labeled telomeric probe, FISH was performed essentially as described by Trask et al. (1991), except PNM buffer was used instead of PN buffer containing 4% goat serum.

Chromosomes were imaged with a Zeiss ICR-35 inverted fluorescence microscope equipped with a 100×/1.4 NA oil immersion lens and a UV filter set, a fluorescein filter set and a fluorescein/rhodamine dual filter set. Photomicrographs were taken with a Canon F12 camera using Kodak Ektachrome™ 400 ASA slide film. Photomicrographs of telomeric signals and DAPI/DA staining were taken at exposure times of 30 s and 10 s, respectively.

In some studies, cells were analyzed by a naive observer to control for potential bias in scoring telomeres. The interchromosomal distribution of detection frequencies in such studies was essentially identical to that in standard analyses.

Southern Analysis of TRF Length

For all HDF strains and cell lines, Southern analysis of terminal restriction fragment (TRF) length was performed as described previously (Allsopp et al., 1992; Allsopp and Harley, 1995), except that the oligonucleotide $(TTAGGG)_3$ was used as a probe instead of $(CCCTAA)_3$.

Results

Telomere Size and Distribution in Interphase Nuclei

Previous measurements of telomere dynamics have typically relied on measurements of the overall distribution of terminal restriction fragment (TRF) lengths. However, sequence analyses of TRFs and analysis of changes in mean TRF length vs loss of signal strength for telomere-binding probes have shown that TRFs consists of both TTAGGG and non-TTAGGG sequences (de Lange et al., 1990; Levy et al., 1992). Fig. 1 illustrates the structure of a typical TRF and the diffuse pattern of TRF sizes detected on a Southern blot by hybridization to a radioactive telomeric oligonucleotide. Analysis of data such as these led to the hypothesis that in the absense of telomerase, critical telomere loss on one or more chromosomes is causally linked to cell cycle exit at senescence (M1) and ultimately to cell death at crisis (M2) (Fig. 1, *A* and *B*, see also Allsopp et al., 1992). At crisis, telomeres may be critically short on nearly all chromosomes (Fig. 1 *B*). Unlike most telomerase-positive immortalized cells which maintain short, stable telomeres postcrisis (Counter et al., 1992, 1994*a*,*b*), many telomerase-negative cells which survive crisis tend to have longer and more heterogeneous TRFs (Fig. 1 *C*).

Since TRF size distributions reflect chromosomal and cellular heterogeneity in both TTAGGG and non-TTAGGG lengths, we decided to use in situ hybridization to analyze changes in telomere size (and interchromosomal variance in telomere size) on an individual cell basis. We examined normal human fibroblasts hybridized in situ with a probe to telomeric DNA by serial optical sectioning and three-dimensional reconstruction by confocal laser scanning microscopy. We found that telomeres are distributed throughout the nuclear volume and are not restricted exclusively to the nuclear periphery (Fig. 2). We found similar results in a variety of human cells in culture (e.g., normal fibroblasts, endothelial cells, transformed fibroblasts, and cancer cell lines) as well as in sections of human tissue (pancreas, thyroid, and muscle) (data not shown). Furthermore, our findings also show that there is heterogeneity in the size of telomeres within interphase nuclei (Fig. 2). There is no apparent relationship between the size of the telomere hybridization signal and the distance of the telomere from the nuclear periphery, indicating that the variance in the size of the spot is not due to accessibility of the probe into the volume of the nucleus.

Changes in Telomere Size during Replicative Aging

Telomeres have been shown to shorten during replicative aging in a variety of human cell types. Interphase FISH analysis of telomeres in cells of the human diploid fibroblast (HDF) strain BJ at various population doubling levels (PDLs) showed a decrease in signal detection frequency, signal intensity, and spot size (all measurements correlated with telomere length) during replicative aging (Fig. 3). Changes in spot size and intensity are apparent over as few as four population doublings (e.g., Fig. 3, *e* and *f*), corresponding to a change in telomere size range of ~200–500 bp. These findings are consistent with the decrease in TRF length and signal intensity with increasing PDL observed in Southern analysis of TRFs from a population of cells (Fig.

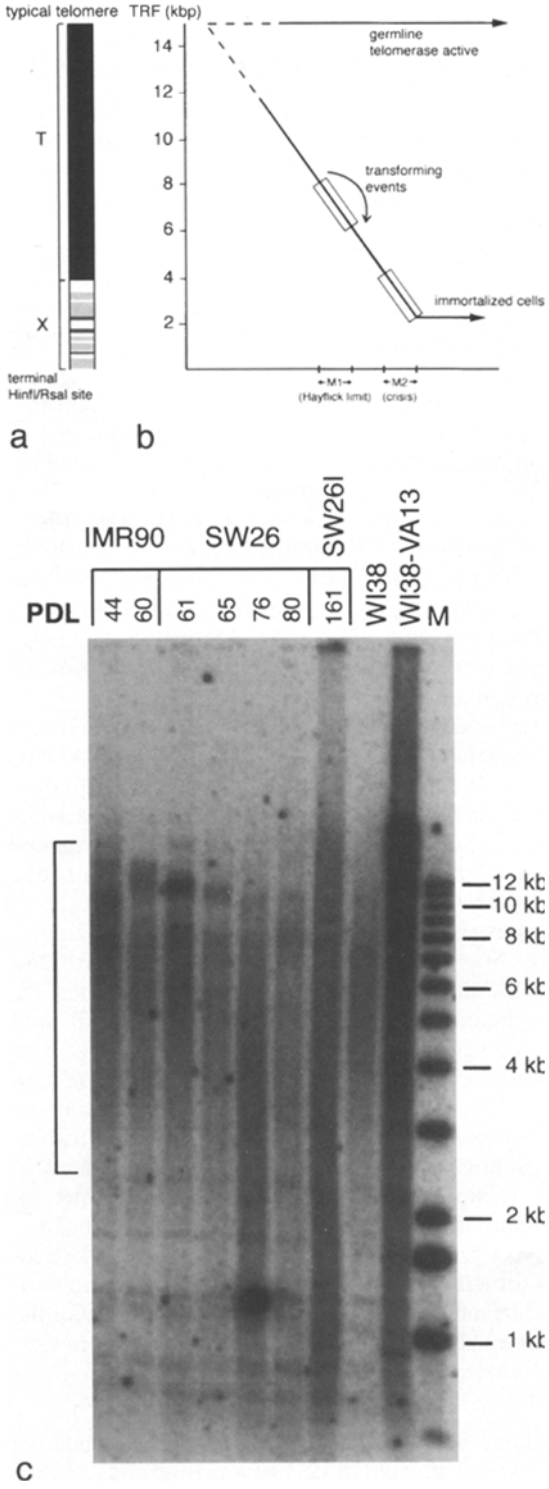

Figure 1. The telomere hypothesis of cell aging and immortalization. (*A*) A model of the sequence composition for a typical TRF is illustrated. The TRF is composed of a terminal (TTAGGG)n tract (T) and a proximal sequence devoid of cleavable restriction sites (X). The X portion of the TRF is likely composed of nontelomeric sequences (*open boxes*), as well as degenerate telomeric sequences (*shaded boxes*) and pure telomeric sequences (*black boxes*). (*B*) Changes in telomere length with increasing population doublings are represented for germ line, normal somatic, and immortalized somatic cells. Telomere length is maintained in germ line cells by telomerase. In contrast, the observed decrease in telomere length in normal somatic cells is consistent with the absence or very low level of telomerase in these cells. At the Hayflick limit (M1), mean TRF length ranges from 6–8 kbp, depending on cell type. We hypothesize that at M1 one or more telomeres have shortened below a critical length required for maintenance of proper telomere structure and function, signaling a check point in cell growth. Mean telomere length (i.e., T) at this point is estimated to be 2–4 kbp. Partially transformed cells which bypass this checkpoint without activation of telomerase continue to lose telomeric DNA until crisis (M2), when cells have critically shortened telomeres on many chromosomes. Cells which survive crisis acquire the ability to maintain or increase telomere length presumably due to genetic alterations. (*C*) Analysis of TRF length during replicative aging of HDF strains and upon immortalization of SV40-transformed HDFs. Genomic DNA was isolated from IMR90, SW26, SW26-i, WI38, and WI38-VA13 cells at the PDLs indicated above each lane and digested with the restriction enzymes HinfI and RsaI. Southern analysis of TRF length was performed as described (Allsopp et al., 1992; Allsopp and Harley, 1995). There exists a broad distribution in TRF size (indicated by bracket in lane *1*) in a cell population due to both interchromosomal heterogeneity and intercellular heterogeneity in the size of both the X and T portion of the TRF (Harley et al., 1990; Levy et al., 1992). Sizes of molecular weight markers are indicated.

1 *C*). In late passage cells, only a minority of the telomeres are detected by FISH and have intensities less than the strongest signals observed in early passage cells (Fig. 3); these signals presumably correspond to the telomeres of chromosomes with the strongest signals in early passage cells. Furthermore, the interchromosomal heterogeneity of the telomere signal persists with aging. These observations suggest a similar rate of loss of telomeric DNA for all chromosomal ends. Also, the remaining detectable telomeric signals in late passage and senescent cells were observed to occur randomly within the nuclear volume, indicating that there is no relationship between the telomere position within the nuclear volume and telomere size or susceptibility to loss of DNA with replicative aging.

Given that all chromosomes appear to lose telomeric DNA at a similar rate and the heterogeneity of telomere signals persist with replicative aging, we attempted to determine if telomere spot size is associated with the end of a specific chromosome. Analysis of young and old fibroblasts hybridized simultaneously with probes to the telomeric repeat and a subtelomeric region of the long arm of chromosome 14 indicated that there is no apparent correlation between the size of the detectable telomeric signal and a specific chromosome end at any given population doubling level (Fig. 4, *a–d*). Similar results were found for the long arm of chromosome 13 (data not shown). This suggests that there is an intercellular heterogeneity of specific chromosome telomeres at any given replicative age (i.e., the telomeres of any particular chromosome may vary in size from cell to cell) in a nonclonal population of cells.

These findings on the changes in size and detectability of individual telomeres with increasing PDL and on the variance in size of individual telomeres at any given PDL are supported by the frequencies of detection of telomeres for particular chromosomes in metaphase spreads. FISH analysis of metaphase chromosomes from early and late passage cells was performed. As was observed in the interphase FISH analysis, telomere signal was reduced at late

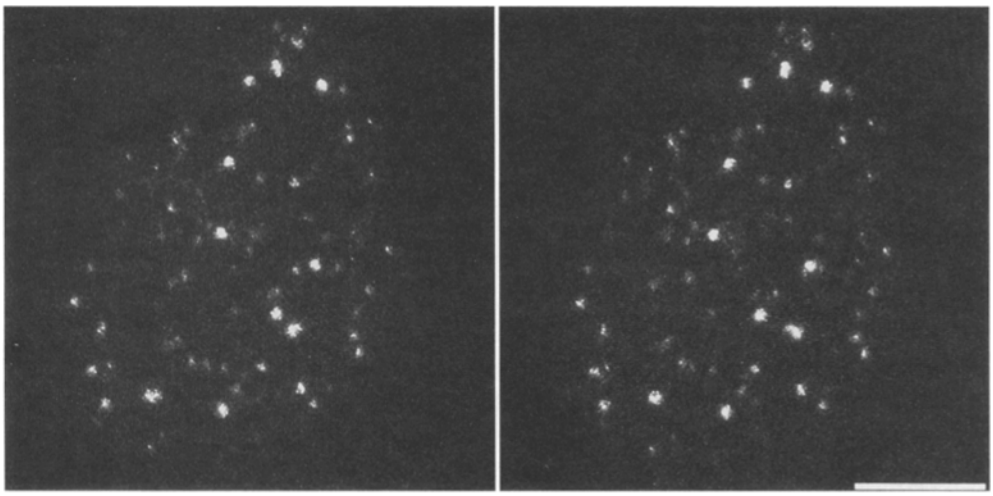

Figure 2. Telomeres of varying sizes are found distributed throughout the nuclear volume. Interphase normal human dermal skin fibroblasts (S2C cells, PDL 38) were hybridized in situ with a FITC-tagged DNA probe complementary to the telomeric repeat. Serial optical sections were taken at 0.5-μm intervals through the depth of the nucleus by confocal laser scanning microscopy. The three-dimensional volume was reconstructed by superimposing the serial images and then the volume images were projected ±6° as a stereo pair. The size of each hybridized telomere spot appears to be independent of its distance from the nuclear periphery or the depth along the z-axis of optical sectioning. This suggests that all regions within the nuclear volume are equally accessible to the hybridization probe and that differences in hybridization spot size reflect differences in telomere size for each of the chromosome ends. Bar, 10 μm.

passage relative to early passage (Fig. 5). Moreover, the detection frequency for telomeres on chromosomes 1, 9, 15, and the Y chromosome as identified by DAPI/DA staining were all less at late passage (Table I). Also, the frequency of detection of telomeric signal varied from telomere to telomere (Table I), which further supports the existence of intracellular heterogeneity in telomere size as indicated by the variability in telomere signal size and intensity observed in interphase cells (Fig. 3). The distribution in telomere size, as indicated by detection frequency, appears to be similar for late passage and early passage cells (Table I), thus providing further evidence for a similar rate of shortening for all telomeres.

Changes in Telomere Size following Cell Transformation

To assess interchromosomal changes in telomere size following transformation, FISH analysis was performed on early and late passage IMR90 cells and the SV40-transformed counterpart cells, both pre- (SW26) and postcrisis (SW26-i). As was found in the analysis of interphase nuclei of other normal fibroblast strains, there was a heterogeneity in the size and distribution of telomere signal within any nucleus as well as an apparent uniform decrease in signal size and intensity with replicative aging (Fig. 6). After transformation, and before crisis, the telomere signal continued to decrease. Similar results were observed in FISH analysis of metaphase chromosomes from IMR90 cells at early passage and SW26 cells near crisis (Table I). As shown in Fig. 6, telomere detectability decreases in SW26 cells near crisis. This observation is in agreement with the short TRF length observed for these cells relative to IMR90 cells at early passage or senescence (Fig. 1 *C*).

In SW26 cells, one copy of chromosome 9 was observed to be associated in a dicentric at a frequency of ~20–30% (R. Allsopp, data not shown). This dicentric appeared to be formed by the end-to-end association, as indicated by the presence of telomeric signal at the junction site, between the long arm of chromosome 9 and another smaller chromosome.

Postcrisis, the detectability of the telomeric signals in SW26-i clones which were telomerase negative (Kim et al., 1994) was very heterogeneous (Fig. 6) (Fig. 4, *i–l*). There was a stabilization of the detectability of telomeric signals in interphase nuclei, and in many cells, the signals increased to sizes and intensities greater than those in the early passage IMR90 cells. A similarly large heterogeneity of telomeric signal was observed in an SV40-transformed WI38 cell line (WI38-VA13) as well (Fig. 4, *e–h*). After performing this analysis on WI38VA13 cells, we discovered, as have others (Bryan et al., 1995), that these cells are also telomerase negative (R. Allsopp, data not shown). Southern analysis of TRF length in these two cell lines also showed a large heterogeneity in telomere length relative to that of the pre-crisis and normal counterpart cells (Fig. 1 *C*). Hybridization with a chromosome specific, subtelomeric probe showed no apparent clustering of telomeric or subtelomeric signals (Fig. 4, *g*, *h*, *k*, and *l*) which argues against the possibility that the large telomeric signals in these cell lines is due to telomere clustering. Also, as was the case for normal HDFs, in a population of cells, there was no apparent relationship between an individual chromosome and its increase in size of the telomeric signal following immortalization, suggesting that the increase in signal is not telomere specific (Fig. 4, *e–l*).

Discussion

Previous analysis, by Southern hybridization, has shown that in somatic cells, the mean TRF length decreases during cell division in vitro and in vivo (Harley et al., 1990; Hastie et al., 1990; Lindsey et al., 1991; Allsopp et al., 1992; Counter et al., 1992; Vaziri et al., 1993, 1994; Chang and Harley, 1995; for a review see Harley and Villeponteau, 1995). These observations are the basis for the hypothesis that, due to the absence of the enzyme telomerase in somatic cells, the shortening of one or more telomeres below a critical length during replicative aging will lead to cell senescence (Harley, 1991). However, these biochemi-

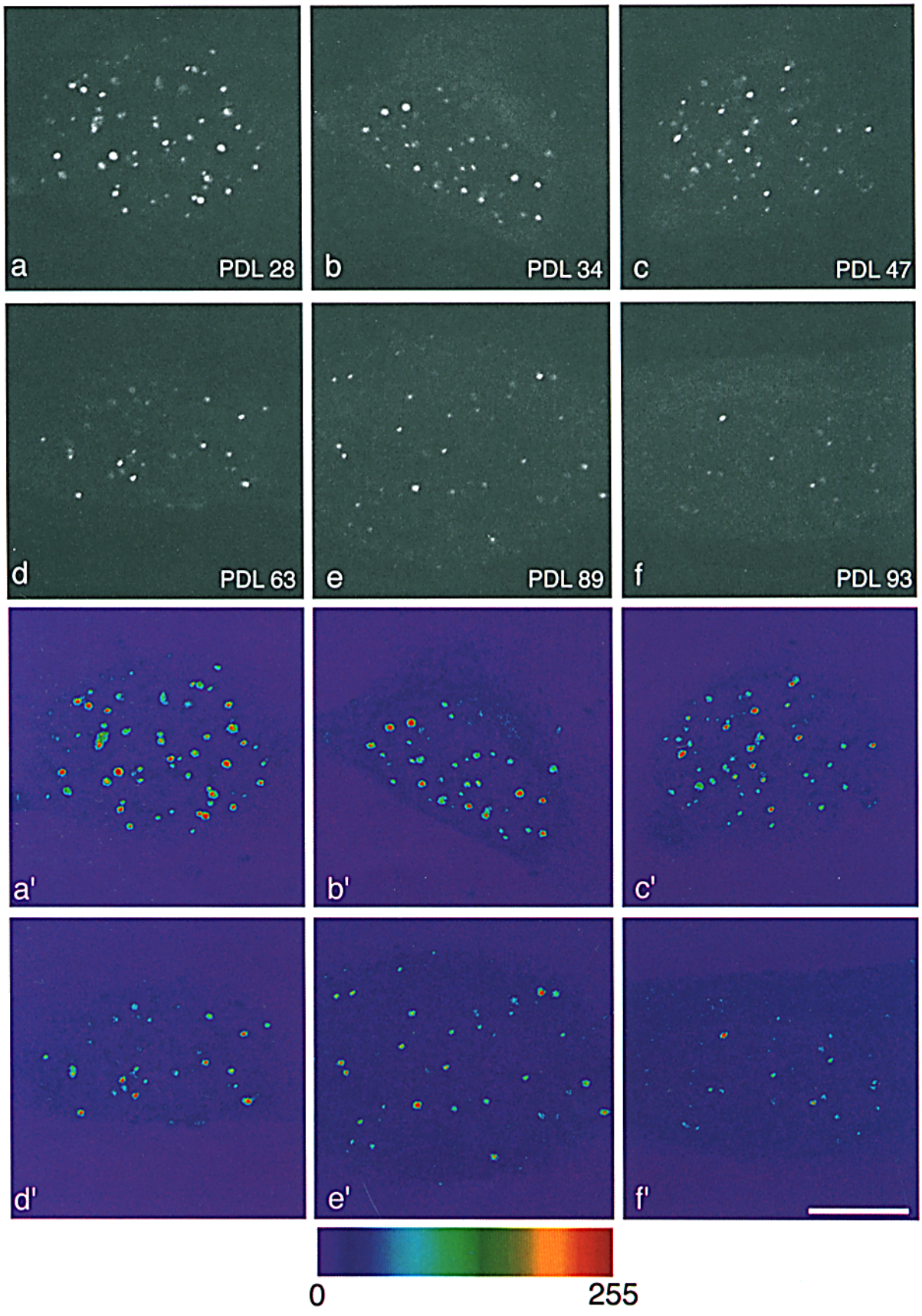
a
PDL 28
b
PDL 34
c
PDL 47
d
PDL 63
e
PDL 89
f
PDL 93
a'
b'
c'
d'
e'
f'
0
255

cal studies were performed on large and often heterogeneous populations of cells. Furthermore, what is measured by Southern analysis is a mean TRF length of all telomeres within the population and thus, makes no allowances for any potential intercellular variability, or more importantly, interchromosomal variability in telomere length or rate of telomere shortening. This study examines the changes in telomere length during replicative aging at the level of single cells and single chromosomes.

Three-dimensional FISH analysis of telomere distribution in interphase HDFs using confocal laser scanning microscopy (CLSM) shows that within the interphase nucleus, telomeres are distributed throughout the nuclear volume. This finding agrees with previous studies by others (Manuelidis and Borden, 1988; Billia and de Boni, 1991; Ferguson and Ward, 1992; Vourc'h et al., 1993; Zalensky et al., 1995) on the non-Rabl distribution of telomeres in mammalian nuclei. These results differ from the localization of telomeres in many plant nuclei, where telomeres are found at one pole of the nucleus (i.e., a "Rabl" configuration) (Anamthawat-Jónsson and Heslop-Harrison, 1990; Rawlins and Shaw, 1990; Rawlins et al., 1991; Schwarzacher and Heslop-Harrison, 1991; Fussell, 1992; Werner et al., 1992). The distribution of telomeres is in all likelihood, not static. Vourc'h et al. (1993) have shown a coordinated movement of centromeres and telomeres relative to the cell cycle in synchronized lymphocytes. The significance of this movement remains to be determined. Possibly, the movement affects the placement of specific subchromosomal regions containing expressed genes in a particular environment in order to facilitate or enhance gene expression at given times during the cell cycle. It has been shown that telomeric DNA binds to nuclear matrix proteins (de Lange, 1992; Markova et al., 1994). Thus, telomeres may act as elements anchoring the chromosomes to the nuclear matrix and/or to other putative intranuclear motors, allowing for coordinated chromosomal movement.

FISH analysis of telomere sizes in interphase cells and on metaphase chromosomes shows that the detectability of individual telomeres in a cell is heterogeneous, suggesting that different telomeres have different lengths. In interphase nuclei, the variability in the distribution of larger vs smaller spots within the nuclear volume countermands the argument that intranuclear differences in hybridization spot size may be related to the penetrability of the probe within the nuclear volume. The probe appears to be equally accessible to the deeper parts of the nuclear volume, suggesting that intranuclear differences in spot size reflect chromosomal differences in telomere size. However, we cannot rule out the possibility of intranuclear and interchromosomal differences in telomeric chromatin structure which may interfere with probe accessibility. It is also possible that the variable detectability is accounted for by interchromosomal differences in the amount of subterminal (TTAGGG)n and telomere-like DNA (see Fig. 1). Brown et al. (1990) and Wells et al. (1990) have examined the interchromosomal distribution of human genomic DNA clones containing telomeric sequences and telomere-like sequences which map to subterminal loci. The distribution of these cloned sequences does not correspond to the distribution of detectable telomeric signals observed in this study, in support of the interpretation that the heterogeneity in detectability of individual telomeres reflects variability in telomere length. However, the distribution of some subterminal sequences has also been shown to be polymorphic (Brown et al., 1990). Additional work using improved methods of measuring true distal (TTAGGG)n length will be required to resolve these issues.

It has been previously shown that the detectability of the sequence probed using FISH correlates with the target size (Lichter et al., 1991). In this study, we have been able to observe changes in telomere size by FISH (i.e., changes in hybridization spot size, intensity, and detectability) over as few as four population doublings in BJ cells. The rate of telomere shortening in these cells is ~40 bp per population doubling (Allsopp, R., unpublished data). Thus, we are able to detect by FISH changes in telomere length as small as ~150 bp. Also, using a similar technique to stain individual telomeres (primed in situ labeling or PRINS), Therkelsen et al. (1995) have observed an inverse correlation between detection frequency of individual telomeres and donor age in human lymphocytes. These observations show that staining of telomeres by FISH and other in situ procedures using fluorescent tags can provide a reliable and sensitive method for detection of changes in telomere length in individual cells.

Both interphase and metaphase FISH analysis show decreases in signal detectability over replicative aging. The persistence of intranuclear heterogeneity of telomere spots (and the corresponding decrease in spot size, intensity, and detectability with time) in interphase FISH analysis, suggests that all telomeres shorten at similar, perhaps equivalent, rates. Also, Southern analysis of TRF length for some HDF strains has revealed that for many HDF strains, the distribution of TRF lengths is multi-modal, where each mode probably reflects a fraction of the telomeres in the genome. The rate of shortening of these modes and of the entire TRF length distribution appear to

Figure 3. The signal from telomeres hybridized in situ decreases in size, intensity, and detectability with replicative aging in culture. BJ cells sampled at population doublings of (*a*) 28, (*b*) 34, (*c*) 47, (*d*) 63, (*e*) 89, and (*f*) 93 were hybridized in situ with a digoxigenin-tagged DNA probe complementary to the telomere repeat and subsequently labeled with rhodamine-tagged anti-digoxigenin antibodies. Single optical sections were taken by confocal laser scanning microscopy through the midplane of each nucleus. FISH analysis was performed at the same time under identical conditions on cells at each PDL. All confocal microscope settings (i.e., brightness, contrast, gain, offset, and pinhole size) were maintained at identical values between each of the samples studied. The heterogeneity in telomere size within any one nucleus persists with replicative aging. However, there is a gradual decrease in spot size, intensity (images *a'–f'*, corresponding to images *a–f*, are color encoded with a 12-step lookup table scaled according to signal intensity) and detectability with replicative aging, such that only the largest telomeres remain detectable in the oldest cells studied. Similar results were obtained for the fibroblast strain S2C (data not shown). Bar, 10 μm.

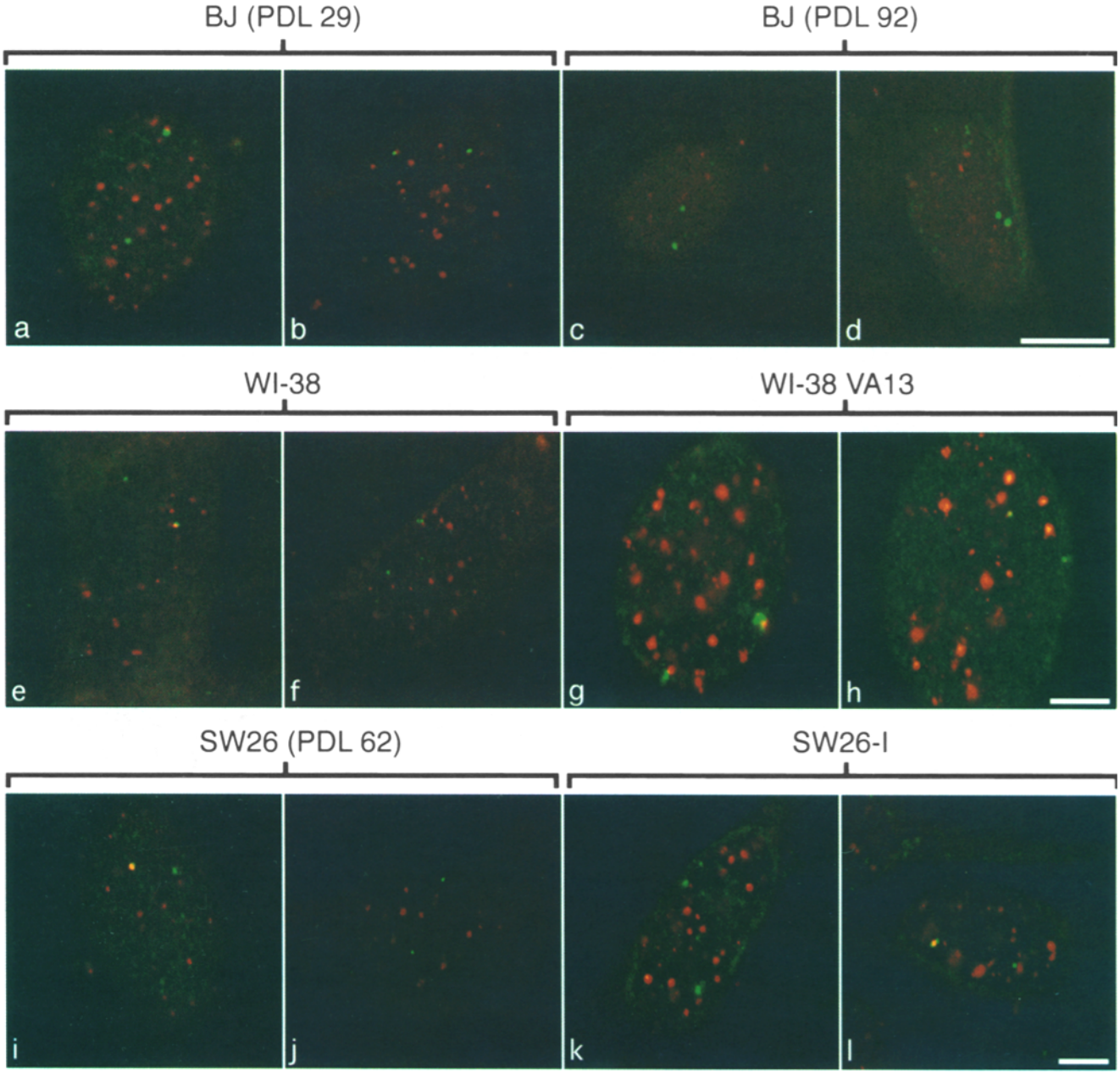

Figure 4. There is no apparent relationship between the long arm of chromosome 14 and the size of the nearest hybridized telomere spot during replicative aging of fibroblasts or following SV40 transformation of fibroblasts. Cells were hybridized in situ with rhodamine-tagged DNA probes complementary to the telomere repeat and digoxigenin-tagged probes to the long arm of chromosome 14. Cells were subsequently labeled with FITC-conjugated antibodies to digoxigenin. Optical sections were taken in each channel (i.e., rhodamine and FITC) at the focal plane of chromosome 14 hybridization. The optical sections showing telomere and chromosome 14 hybridization were superimposed and pseudocolored. In nonclonal populations of young (*a* and *b*) and old (*c* and *d*) fibroblasts (BJ cells), there appears to be no correlation between the end of the long arm of chromosome 14 and the size of the nearest telomere spot, indicating an intercellular heterogeneity of chromosome-specific telomeres at any given replicative age. In random nonclonal populations of normal fibroblasts (WI-38) (*e* and *f*) and SV40 immortalized counterparts (WI-38 VA13) (*g* and *h*), there appears to be no correlation between the end of the long arm of chromosome 14 and the size of the nearest telomere spot. No apparent relationship was observed between the long arm of chromosome 14 and the size of the nearest hybridized telomere spot either before (*i* and *j*) or after (*k* and *l*) crisis in SV40-transformed IMR90 fibroblasts. This intercellular heterogeneity in telomere size for 14q suggests that telomere amplification after a crisis is not chromosome-specific. Bars, 10 μm.

be similar (Allsopp and Harley, 1995 and Prowse, K., personal communication), providing further evidence that the rate of shortening is similar for all telomeres. However, our study does not reveal whether the telomeres with a strong or weak signal in a specific cell at early passage give rise to telomeres with a correspondingly strong or weak signal in senescent cells. The simultaneous analysis of all 92 telomeres in the human genome in clonal cell popula-

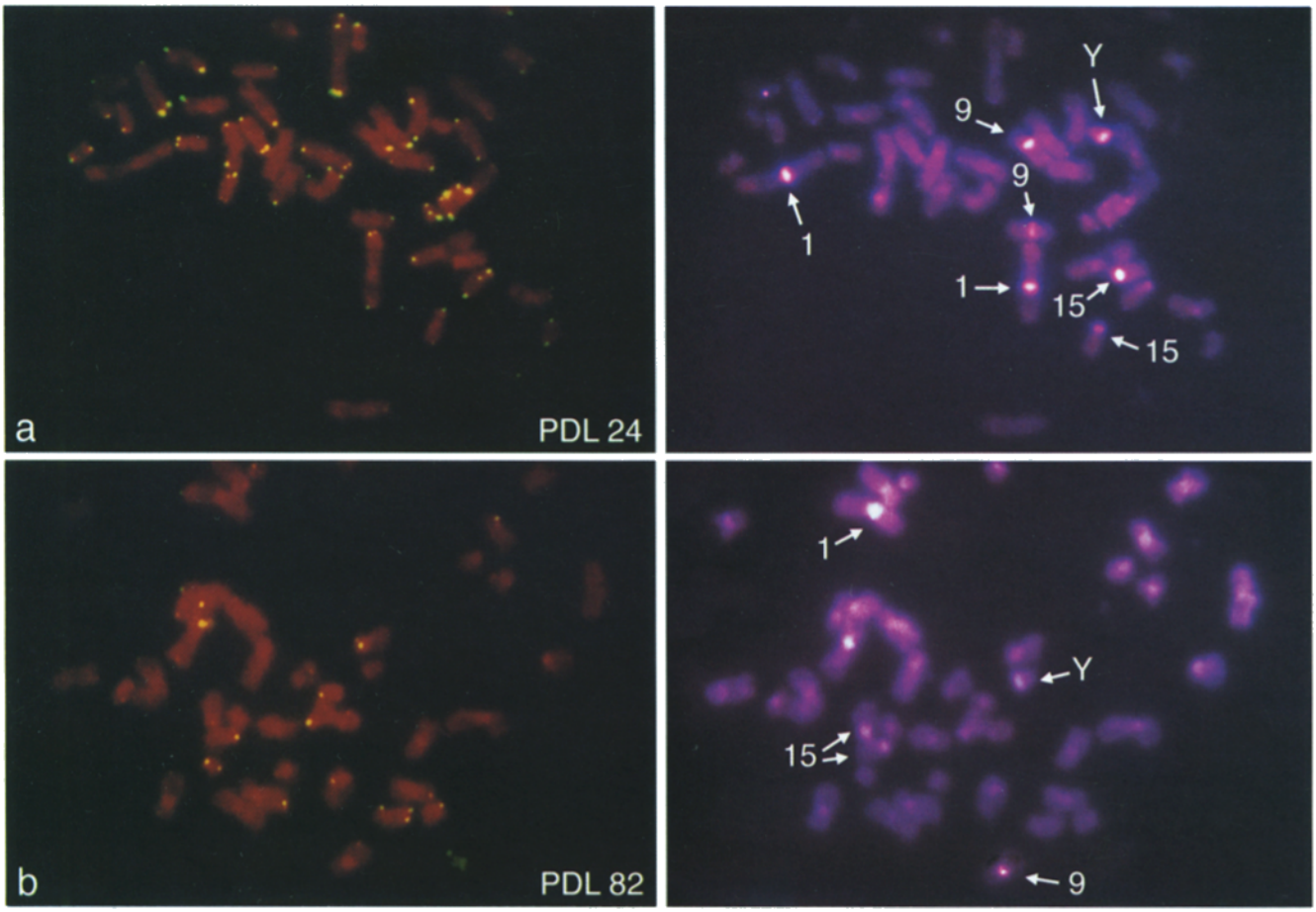

Figure 5. Telomere detectability decreases on individual metaphase chromosomes during replicative aging of the HDF strain BJ. Metaphase spreads prepared from BJ cells at (*a*) early passage (PDL 24) and (*b*) late passage (PDL 82) were hybridized in situ with a digoxigenin-tagged telomeric DNA probe, and the signal was amplified and subsequently detected with FITC-conjugated anti-digoxigenin antibodies as described in Materials and Methods. FISH analysis was performed at the same time under identical conditions for cells at each PDL. Photomicrographs showing telomeric signal (*left*) and DAPI/DA staining (*right*) are shown. Chromosomes 1, 9, 15, and the Y chromosome as identified by DAPI/DA staining are indicated.

tions will provide stronger evidence as to whether all telomeres shorten at equivalent rates.

The large interchromosomal heterogeneity in telomeric signal intensity in the SV40 immortalized SW26i and WI38VA13 cells correlates with an absence of detectable telomerase in these cells (Kim et al., 1994; Bryan et al., 1995 and data not shown). Also, other studies indicate that there is an association between a lack of telomerase activity and large heterogeneity in TRF lengths in human cell lines immortalized using SV40 or by other means (Murnane et al., 1994; Bryan et al., 1995). In contrast, telomerase-positive 293 cells have shorter, more homogeneous TRF lengths and FISH telomere signals (Henderson, S., and R. Allsopp, data not shown). However, the composition of the TRFs in telomerase-negative cell lines is unknown. The data presented here suggest that the large heterogeneity in TRF length in telomerase-negative cell lines is accounted for by variability of the size of the terminal TTAGGG tract. The alternative possibility is that degenerate TTAGGG sequences of variable lengths, perhaps in combination with pure TTAGGG sequences, have been added on to the telomeric termini in these cells. Additional work will be required to determine the exact composition and mechanism of synthesis of the telomeric DNA in telomerase-negative immortal cells and also to determine whether large intracellular heterogeneity in telomere length is unique to these cells.

Two predictions of the telomere hypothesis are (*1*) the shortening of one or more telomeres below a critical length, Tc, will induce cell senescence, and (*2*) the accumulation of critically shortened telomeres to a threshold level will initiate crisis in transformed cells which have bypassed cell senescence (Harley, 1991). We have previously calculated the mean telomere length at senescence, which provides an upper estimate of Tc, to be ~2–4 kbp (Allsopp and Harley, 1995 and unpublished data). However, if interchromosomal heterogeneity in telomere length exists as suggested in this study, then Tc will be less than the mean telomere length. Since there is a large distribution of lengths for each individual telomere in a cell population at any given PDL (Prowse, K., personal communication), it is even possible that cell senescence may be induced by the complete loss of telomeric DNA from the ends of one or a few chromosomes.

Table I. Quantitative Analysis of Telomeric Signal on Individual Metaphase Chromosomes for Early and Late Passage BJ Cells, Early Passage IMR90 Cells, and SW26 Cells Near Crisis

	Percent detectability*							
	1		9		15		Y	
Chromosome	p	q	p	q	p	q	p	q
Early passage‡	88**	74	68	78	89	60	85	54
Late passage§	58	43	32	44	76	40	48	27
IMR90‡	79¶	84	86	71	87	72	–	–
SW26¶	39	39	37	26	58	30	–	–

*Chromosomes were identified by DAPI/DA staining. Although chromosome 16 is also identified by DAPI/DA staining, percent detectability of telomeric signals was not assessed for this chromosome due to difficulty in distinguishing between the long and short arms.

‡The percent detectability is significantly less for early passage BJ cells and IMR90 cells than for late passage BJ cells and SW26 cells, respectively ($P < 0.0001$, paired t test).

§Late passage cells were analyzed at PDL 75-82.

¶SW26 cells were analyzed at PDL 63. Crisis occurred at PDL 66.

**Values were calculated using data from five experiments using either a biotinylated telomeric probe or a digoxigenin-labeled probe (qualitatively similar results were obtained for both probes).

A critically short telomere may be analogous to a double-stranded DNA break. Recently, di Leonardo et al. (1994) provided evidence suggesting that the presence of a single double-stranded DNA break in a cell is capable of inducing irreversible cell cycle arrest in human cells. Thus, replicative senescence may be initiated by the signaling of a DNA damage pathway. Furthermore, chromosome ends which lack telomeres are highly fusogenic, and therefore the accumulation of critically shortened telomeres in senescent and transformed cells could explain the accumulation of dicentric chromosomes in these cells (Benn, 1976; Sherwood et al., 1989; Counter et al., 1992, 1994*a*). This prediction is supported by the preliminary observations that the telomere on 9q appears to be relatively short in IMR90 and SW26 cells (Table I), and that one copy of chromosome 9 is frequently engaged in an end-to-end dicentric involving 9q in SW26 cells (R. Allsopp, data not shown). Additional work will be required to confirm whether or not chromosomes with short telomeres engage in end-to-end associations more frequently than chromosomes with long telomeres.

In summary, FISH has been shown to be a sensitive and useful method for detecting changes in length of individual telomeres and for semiquanitative analysis of the relative lengths of individual telomeres. The data from analysis of individual cells supports the previously observed loss of telomeric DNA during replicative aging as detected by Southern analysis of TRFs. Furthermore, it indicates that

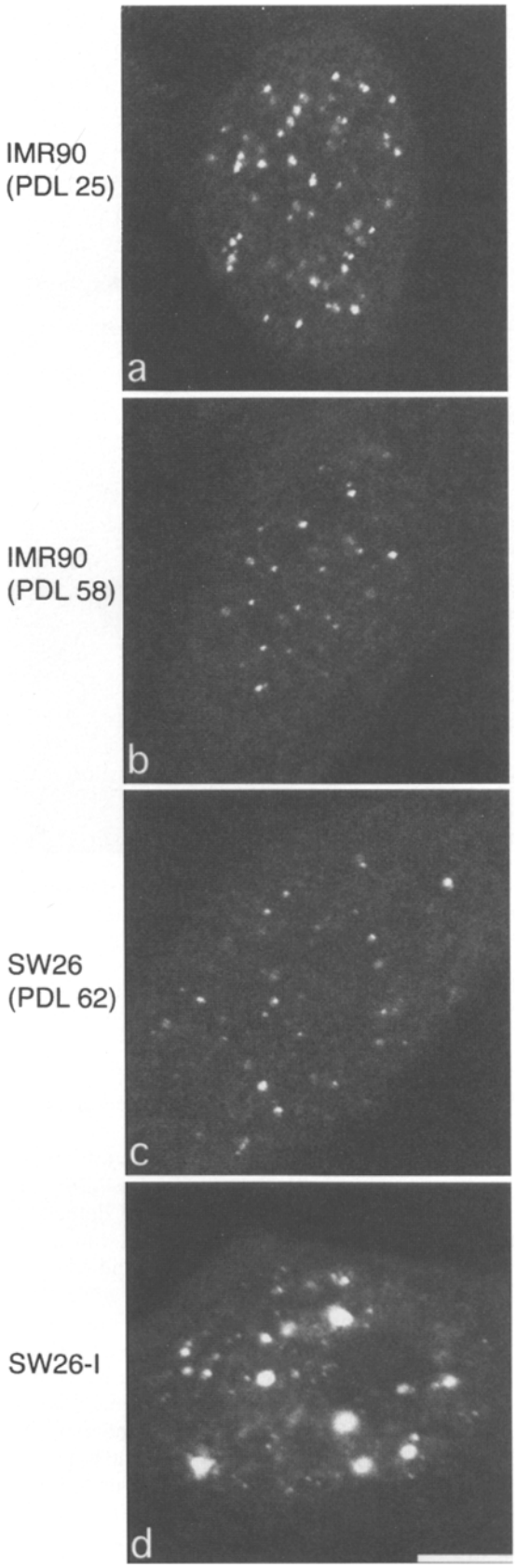

Figure 6. Telomere size stabilizes, and in some cases, increases in transformed cells following immortalization. Optical sections generated by confocal laser scanning microscopy show that telomere hybridization signals (as detected by FISH of digoxigenin-tagged telomeric DNA probes) decrease in size, intensity, and detectability in IMR90 fibroblasts with replicative aging (*a*, early, PDL 25; *b*, late, PDL 58). After SV40 transfection, and before crisis, telomeres further decrease in size (*c*, SW26 cells, PDL 62). After crisis, in the immortalized cell line, telomeres are seen to maintain or increase (*d*, SW26-I cells) in size. FISH analysis was performed at the same time under identical conditions for both cell strains. A similar increase in telomere size is observed in SV40-transformed WI-38 fibroblasts (Fig. 4, *e–h*). Bar, 10 μm.

all telomeres shorten at similar, perhaps equivalent, average rates and that different telomeres have different lengths. Analysis of telomere lengths by FISH may be particularly useful when dealing with small cell populations or heterogeneous cell populations, including tissues. Furthermore, interphase FISH may prove useful in analysis of telomere length in small populations of cells that do not divide or divide infrequently. Thus, FISH has diagnostic applications for analysis of telomere length, replicative age, and remaining replicative capacity in somatic cells, including stem cells, in both normal and diseased states.

The authors are grateful to Woody Wright and Jerry Shay for kindly providing the plasmid pBLrep4 and to John Murnane for providing the plasmid pEE3A. We also thank Choy-Pik Chiu for helpful comments on the manuscript.

This study was supported by grants to C.B. Harley from the National Institutes of Health (AG-09383) as well as the Allied Signal Award (C.B. Harley). S.C. Henderson and D.L. Spector were funded by grants from the Culpeper Foundation and the Council for Tobacco Research (3295R1). R.C. Allsopp holds a Medical Research Council of Canada Studentship.

Received for publication 23 January 1996 and in revised form 17 April 1996.

References

Allshire, R.C., M. Dempster, and N.D. Hastie. 1989. Human telomeres contain at least three types of G-rich repeat distributed non-randomly. *Nucleic Acids Res.* 17:4611–4627.

Allsopp, R.C., and C.B. Harley. 1995. Evidence for a critical telomere length in senescent human fibroblasts. *Exp. Cell Res.* 219:130–136.

Allsopp, R.C., H. Vaziri, C. Patterson, S. Goldstein, E.V. Younglai, A.B. Futcher, C.W. Greider, and C.B. Harley. 1992. Telomere length predicts replicative capacity of human fibroblasts. *Proc. Natl. Acad. Sci. USA.* 89: 10114–10118.

Anamthawat-Jónsson, K., and J.S. Heslop-Harrison. 1990. Centromeres, telomeres and chromatin in the interphase nucleus of cereals. *Caryologia.* 43: 205–213.

Benn, P.A. 1976. Specific chromosome aberrations in senescent fibroblast cell lines derived from human embryos. *Am. J. Human Genet.* 28:465–473.

Billia, F., and U. de Boni. 1991. Localization of centromeric satellite and telomeric DNA sequences in dorsal root ganglion neurons, in vitro. *J. Cell Sci.* 100:219–226.

Blackburn, E.H. 1991. Structure and function of telomeres. *Nature (Lond.).* 350:569–573.

Bourgain, F.M., and M.D. Katinka. 1991. Telomeres inhibit end to end fusion and enhance maintenance of linear DNA molecules injected into the *Paramecium primaurelia* macronucleus. *Nucleic Acids Res.* 19:1541–1547.

Broccoli, D., J.W. Young, and T. de Lange. 1995. Telomerase activity in normal and malignant hematopoietic cells. *Proc. Natl. Acad. Sci. USA.* 92:9082–9086.

Brown, W.R.A., P.J. MacKinnon, A. Villasanté, N. Spurr, V.J. Buckle, and M.J. Dobson. 1990. Structure and polymorphism of human telomere-associated DNA. *Cell.* 63:119–132.

Bryan, T.M., A. Englezou, J. Gupta, S. Bacchetti, and R.R. Reddel. 1995. Telomere elongation in immortal human cells without detectable telomerase activity. *EMBO (Eur. Mol. Biol. Organ.) J.* 14:4240–4248.

Chang, E., and C.B. Harley. 1995. Telomere length and replicative aging in human vascular tissues. *Proc. Natl. Acad. Sci. USA.* 92:11190–11194.

Chiu, C. P., W. Dragowska, N.W. Kim, H. Vaziri, J. Yui, T.E. Thomas, C.B. Harley, and P.M. Lansdorp. 1996. Differential expression of telomerase activity in hemopoietic progenitors from adult human bone marrow. *Stem Cells.* 14:239–248.

Counter, C.M., A.A. Avilion, C.E. LeFeuvre, N.G. Stewart, C.W. Greider, C.B. Harley, and S. Bacchetti. 1992. Telomere shortening associated with chromosome instability is arrested in immortal cell which express telomerase activity. *EMBO (Eur. Mol. Biol. Organ.) J.* 11:1921–1929.

Counter, C.M., F.M. Botelho, P. Wang, C.B. Harley, and S. Bacchetti. 1994*a*. Stabilization of short telomeres and telomerase activity accompany immortalization of Epstein-Barr virus-transformed human B lymphocytes. *J. Virol.* 68:3410–3414.

Counter, C.M., H.W. Hirte, S. Bacchetti, and C.B. Harley. 1994*b*. Telomerase activity in human ovarian carcinoma. *Proc. Natl. Acad. Sci. USA.* 91:2900–2904.

Counter, C.M., J. Gupta, C.B. Harley, B. Leber, and S. Bacchetti. 1995. Telomerase activity in normal leukocytes and in hematologic malignancies. *Blood.* 85:2315–2320.

de Lange, T. 1992. Human telomeres are attached to the nuclear matrix. *EMBO (Eur. Mol. biol. Organ.) J.* 11:717–724.

de Lange, T., L. Shiue, R. Myers, D.R. Cox, S.L. Naylor, A.M. Killery, and H.E. Varmus. 1990. Structure and variability of human chromosome ends. *Mol. Cell. Biol.* 10:518–527.

Dell'Orco, R.T., J.G. Mertens, and P.F. Kruse. 1973. Doubling potential, calendar time, and senescence of human diploid cells in culture. *Exp. Cell Res.* 77: 356–360.

di Leonardo, A., S.P. Linke, K. Clarkin, and G.M. Wahl. 1994. DNA damage triggers a prolonged p53-dependent G_1 arrest and long-term induction Cip1 in normal human fibroblasts. *Genes Dev.* 8:2540–2551.

Feng, J., W.D. Funk, S.-S. Wang, S.L. Weinrich, A.A. Avilion, C.-P. Chiu, R.R. Adams, E. Chang, R.C. Allsopp, J. Yu, et al. 1995. The RNA component of human telomerase. *Science (Wash. DC).* 269:1236–1241.

Ferguson, M., and D.C. Ward. 1992. Cell cycle dependent chromosomal movement in pre-mitotic human T-lymphocyte nuclei. *Chromosoma.* 101:557–565.

Finch, C.E. 1990. Longevity, Senescence and the Genome. University of Chicago Press, Chicago, IL. 416–423.

Fussell, C.P. 1992. Rabl distribution of interphase and prophase telomeres in *Allium cepa* not altered by colchicine and/or ultracentrifugation. *Am. J. Botany.* 79:771–777.

Gilson, E., T. LaRoche, and S.M. Gasser. 1993. Telomeres and the functional architecture of the nucleus. *Trends Cell Biol.* 3:128–134.

Goldstein, S. 1974. Aging in vitro: growth of cultured cells from the Galapagos tortoise. *Exp. Cell Res.* 83:297–302.

Goldstein, S. 1990. Replicative senescence: the human fibroblast comes of age. *Science (Wash. DC).* 249:1129–1133.

Greider, C.W., and E.H. Blackburn. 1985. Identification of a specific telomere terminal transferase activity in *Tetrahymena* extracts. *Cell.* 43:405–413.

Greider, C.W., and E.H. Blackburn. 1989. A telomeric sequence in the RNA of *Tetrahymena* telomerase required for telomere repeat synthesis. *Nature (Lond.).* 337:331–337.

Harley, C.B. 1991. Telomere loss: mitotic clock or genetic time bomb? *Mutat. Res.* 256:271–282.

Harley, C.B., and B. Villeponteau. 1995. Telomeres and telomerase in aging and cancer. *Curr. Opin. Genet. Dev.* 5:249–255.

Harley, C.B., A.B. Futcher, and C. W. Greider. 1990. Telomeres shorten during aging of human fibroblasts. *Nature (Lond.).* 345:458–460.

Hastie, N.D., M. Dempster, M.G. Dunlop, A.M. Thompson, D.K. Green, and R.C. Allshire. 1990. Telomere reduction in human colorectal carcinoma and with aging. *Nature (Lond.).* 346:866–868.

Hayflick, L., and P. Moorhead. 1961. The serial cultivation of human diploid cell strains. *Exp. Cell Res.* 25:585–621.

Henderson, E.R., M. Moore, and B. A. Malcolm. 1990. Telomere G-strand structure and function analyzed by chemical protection, base analogue substitution, and utilization by telomerase in vitro. *Biochemistry.* 29:732–737.

Hiyama, E., K. Hiyama, T. Yokohama, Y. Matsuura, M.A. Piatyszek, and J.W. Shay. 1995. Correlating telomerase activity levels with human neuroblastoma outcomes. *Nature Med.* 1:249–255.

Johnson, G.D., and G.M.d.C. Nogueira Araujo. 1981. A simple method of reducing the fading of immunofluorescence during microscopy. *J. Immun. Methods.* 43:349–350.

Kim, N.W., M.A. Piatyszek, K.R. Prowse, C.B. Harley, M.D. West, P.L.C. Ho, G.M. Coviello, W.E. Wright, S.L. Weinrich, and J.W. Shay. 1994. Specific association of human telomerase activity with immortal cells and cancer. *Science (Wash. DC).* 266:2011–2015.

Langer, P.R., A.A. Waldrop, and D.C. Ward. 1981. Enzymatic synthesis of biotin labeled polynucleotides: novel nucleic acid affinity probes. *Proc. Natl. Acad. Sci. USA.* 78:6633–6637.

Levy, M.Z., R.C. Allsopp, A.B. Futcher, C.W. Greider, and C.B. Harley. 1992. Telomere end-replication problem and cell aging. *J.Mol. Biol.* 225:951–960.

Lichter, P., A.L. Boyle, T. Cremer, and D.C. Ward. 1991. Analysis of genes and chromosomes by nonisotopic in situ hybridization. *GATA.* 8:24–35.

Lindsey, J., N.I. McGill, L.A. Lindsey, D.K. Green, and H.J. Cooke. 1991. In vivo loss of telomeric repeats with age in humans. *Mutat. Res.* 256:45–48.

Lundblad, V., and J.W. Szostak. 1989. A mutant with a defect in telomere elongation leads to senescence in yeast. *Cell.* 57:633–643.

Manuelidis, L., and J. Borden. 1988. Reproducible compartmentalization of individual chromosome domains in human CNS cells revealed by in situ hybridization and three-dimensional reconstruction. *Chromosoma.* 96:397–410.

Markova, D., R. Donev, C. Patriotis, and L. Djondjurov. 1994. Interphase chromosomes of Friend-S cells are attached to the matrix structures through the centromeric/telomeric regions. *DNA Cell Biol.* 13:941–951.

Martin, G.M., C.M. Sprague, and E.J. Epstein. 1970. Replicative life-span of cultivated human cells. *Lab. Invest.* 23:86–92.

McClintock, B. 1941. The stability of broken chromosomes in *Zea mays*. *Genetics.* 41:234–282.

Meyne, J., R.L. Ratliff, and R.K. Moyzis. 1989. Conservation of the human telomere sequence (TTAGGG)n among vertebrates. *Proc. Natl. Acad. Sci. USA.* 86:7049–7053.

Moyzis, R.K., J.M. Buckingham, L.S. Cram, M. Dani, L.L. Deaven, M.D. Jones, J. Meyne, R.L. Ratliff, and J.R. Wu. 1988. A highly conserved repetitive DNA sequence, $(TTAGGG)_n$, present at the telomeres of human chromosomes. *Proc. Natl. Acad. Sci. USA.* 85:6622–6626.

Muller, H.J. 1938. The remaking of chromosomes. *Collecting Net.* 13:182–193.
Murnane, J.P., and L.-C. Yu. 1993. Acquisition of telomere repeat sequences by transfected DNA integrated at the site of a chromosomal break. *Mol. Cell. Biol.* 13:977–983.
Murnane, J.P., L. Sabatier, B.A. Marder, and W.F. Morgan. 1994. Telomere dynamics in an immortal human cell line. *EMBO (Eur. Mol. Biol. Organ.) J.* 13:4953–4962.
Olovnikov, A.M. 1971. Principle of marginotomy in template synthesis of polynucleotides. *Dokl. Acad. Nauk. S.S.S.R.* 201:1496–1499.
Olovnikov, A.M. 1973. A theory of marginotomy. The incomplete copying of template margin in enzymic synthesis of polynucleotides and biological significance of the phenomenon. *J. Theor. Biol.* 41:181–190.
Rawlins, D.J., and P.J. Shaw. 1990. Localization of ribosomal and telomeric DNA sequences in intact plant nuclei by *in situ* hybridization and three-dimensional optical microscopy. *J. Micros.* 157:83–89.
Rawlins, D.J., M.I. Highett, and P.J. Shaw. 1991. Localization of telomeres in plant interphase nuclei by in situ hybridization and 3D confocal microscopy. *Chromosoma.* 100:424–431.
Sandell, L., and V.A. Zakian. 1993. Loss of a yeast telomere: arrest, recovery, and chromosome loss. *Cell.* 75:729–739.
Schwarzacher, T., and J.S. Heslop-Harrison. 1991. *In situ* hybridization to plant telomeres using synthetic oligomers. *Genome.* 34:317–323.
Schweizer, D., P. Ambros, and M. Andrle. 1978. Modification of DAPI banding on human chromosomes by prestaining with a DNA-binding oligopeptide antibiotic, distamycin A. *Exp. Cell. Res.* 111:327–332.
Sen, D., and W. Gilbert. 1988. Formation of parallel four-stranded complexes by guanine-rich motifs in DNA and its implications for meiosis. *Nature (Lond.).* 334:410–414.
Sherwood, S., D. Rush, J.L. Ellsworth, and R.T. Schimke. 1989. Defining cellular senescence in IMR-90 cells: a flow cytometric analysis. *Proc. Natl. Acad. Sci. USA.* 85:9086–9090.
Stanulis-Praeger, B. 1987. Cellular senescence revisited: a review. *Mech. Ageing Dev.* 38:1–48.
Therkelsen, A.J., A. Nielsen, J. Koch, J. Hindkjær, and S. Kølvraa. 1995. Staining of human telomeres with primed *in situ* labeling (PRINS). *Cytogenet. Cell Genet.* 68:115–118.
Tommerup, H., A. Dousmanis, and T. de Lange. 1994. Unusual chromatin in human telomeres. *Mol. Cell. Biol.* 14:5777–5785.
Trask, B.J., H. Massa, S. Kenwrick, and J. Gitschier. 1991. Mapping of human chromosome Xq28 by two-color fluorescence in situ hybridization of DNA sequences to interphase cell nuclei. *Am. J. Hum. Genet.* 48:1–15.
Vaziri, H., W. Dragowska, R.C. Allsopp, T.E. Thomas, C.B. Harley, and P.M. Lansdorp. 1994. Evidence for a mitotic clock in human hemopoietic stem cells: loss of telomeric DNA with age. *Proc. Natl. Acad. Sci. USA.* 91:9857–9860.
Vaziri, H., F. Schaechter, I. Uchida, W.L., Z. Xiaoming, R. Effros, D. Choen, and C.B. Harley. 1993. Loss of telomeric DNA during aging of normal and trisomy 21 human lymphocytes. *Am. J. Hum. Genet.* 52:661–667.
Vourc'h, C., D. Taruscio, A.L. Boyle, and D.C. Ward. 1993. Cell cycle-dependent distribution of telomeres, centromeres, and chromosome-specific subsatellite domains in the interphase nucleus of mouse lymphocytes. *Exp. Cell Res.* 205:142–151.
Watson, J.D. 1972. Origin of concatemeric T7 DNA. *Nature New Biol.* 239: 197–201.
Weber, B., C. Collins, C. Robbins, R.E. Magenis, A.D. Delaney, J.W. Gray, and M.R. Hayden. 1990. Characterization and organization of DNA sequences adjacent to the human telomere associated repeat (TTAGGG)n. *Nucleic Acids Res.* 18:3353–3361.
Wells, R.A., G.G. Germino, S. Krishna, V.J. Buckle, and S.T. Reeders. 1990. Telomere-related sequences at interstitial sites in the human genome. *Genomics.* 8:699–704.
Weng, N.-P., B. Levine, B.L. June, and R.J. Hodes. 1995. Human naive and memory T lymphocytes differ in telomeric length and replicative potential. *Proc. Natl. Acad. Sci. USA.* 92:11091–11094.
Werner, J.E., R.S. Kota, B.S. Gill, and T.R. Endo. 1992. Distribution of telomeric repeats and their role in the healing of broken chromosome ends in wheat. *Genome.* 35:844–848.
Wright, W.E., and J.W. Shay. 1995. Time, telomeres and tumours: is cellular senescence more than an anticancer mechanism? *Trends Cell Biol.* 5:293–297.
Zalensky, A.O., M.J. Allen, A. Kobayashi, I.A. Zalenskaya, R. Balhorn, and E.M. Bradbury. 1995. Well-defined genome architecture in the human sperm nucleus. *Chromosoma.* 103:577–590.